A ROS-responsive drug-conjugated heparin biomimetic nanogel for enhancing anticoagulant, antibacterial, and anti-calcification properties of bioprosthetic heart valves

Ming Chen,[†a,b] Shufen Li,[†a,c] Tianyi Qu,[a,c] Zheng Chai,[a,b] Ying Zhang,[a,b] Yongchao Yao,[d] Weihua Zhuang,[*c,d] Wenchuang (Walter) Hu[d] and Mao Chen[*a,b,c]

[a] Laboratory of Cardiac Structure and Function, Institute of Cardiovascular Diseases, West China Hospital, Sichuan University, Chengdu, 610041, China.

[b] Department of Cardiology, West China Hospital, Sichuan University, Chengdu, 610041, China.

[c] Cardiac Structure and Function Research Key Laboratory of Sichuan Province, West China Hospital, Sichuan University, Chengdu, 610041, China.

[d] Precision Medicine Translational Research Center, West China Hospital, Sichuan University, Chengdu 610041, China.

[†]Ming Chen and Shufen Li contributed equally to this work.

[*] Corresponding author, Email address: chenmao@scu.edu.cn and weihuaz@scu.edu.cn.

Experimental

Experimental

Materials

Ofloxacin, N,N-dimethylpyridin-4-aMine 4-methylbenzenesulfonate (DMAP. TsOH salt), O-benzotriazole-N,N,N',N'-tetramethyl-uronium-hexafluorophosphate (HBTU) and dicyclohexylcarbodiimide (DCC) were purchased from Bide Pharmatech, Ltd. (Shanghai, China). Methacryloyl chloride, 2-acrylamide-2-methylpropanesulfonic acid (AMPS), N,N'-methylenebisacrylamide (MBAA), N-acryloxysuccinimide (NAS), sodium dodecyl sulfate, sodium deoxycholate, N-acetoxysuccinimide, and 3-(4,5-dimethylthiazol-2-yl)-2,5-diphenyltetrazolium bromide (MTT) were purchased from Adamas Reagent, Ltd. (Shanghai, China). DCFH-DA and lipopolysaccharide (LPS) were purchased from Sigma-Aldrich (St. Louis, MO, USA). Mouse TNF-α ELISA kit was purchased from Cloud-Clone Corp. (Wuhan, China). The primary antibodies antibodies used in the immunofluorescence experiments are as follows: CD86 (1:1000, Aifang Biological, China) and CD206 (1:1000, Aifang Biological, China). Fluorescein diacetate (FDA), DMAO, PI, and CCK-8 kits were purchased from Yeasen Biotechnology Co., Ltd. (Shanghai, China). 1-Ethyl-3-(3-dimethylaminopropyl) carbodiimide (EDC), N-hydroxy succinimide (NHS), branched poly(ethyleneimine) (PEI) (M_w = 25,000), and 50% glutaraldehyde solutions were purchased from Titan Scientific Co., Ltd. (Shanghai, China). 2,2-Azobisisobutyronitrile (AIBN) was purchased from Sigma Aldrich. Collagenase type II, Dulbecco's modified Eagle's medium (DMEM) and fetal bovine serum (FBS) were purchased from Gibco (Thermo Fisher Scientific, USA). All the chemicals and solvents were used as received without further purification.

Preparation of Glut

Fresh bovine pericardial tissues were infiltrated with an aqueous solution comprising 0.5% (w/v) sodium dodecyl sulfate and 0.1% (w/v) sodium deoxycholate for 12 h with continuous shaking at 4 °C. Subsequently, the decellularized pericardia were rinsed with saline and crosslinked with 1% (w/v) glutaraldehyde solution for 48 h to obtain Glut.

Characterization of NP and NP-OFL

FTIR spectra of NP, MC-TK-OFL, and NP-OFL were acquired using an attenuated total reflection Fourier transform infrared spectrometer (ATR-FTIR, Thermo Fisher Scientific Nicolet iS50) to confirm the successful introduction of MC-TK-OFL into the nanogel. NP and NP-OFL solutions were prepared in phosphate-buffered saline (PBS). The particle size distributions and zeta potentials of NP and NP-OFL were determined via dynamic light scattering (DLS) on a Zetasizer Pro (ZSU3200). The stability of the nanogels was detected by monitoring the particle size via DLS at different times. The

morphology of the NP and NP-OFL was observed by scanning electron microscopy (SEM, Thermo Fisher Scientific Apreo 2S).

Drug loading content of NP-OFL

The absorbance of the centrifuged supernatant was measured with a UV spectrophotometer. The concentration of MC-TK-OFL retrieved from the centrifuged supernatant was subsequently calculated according to the standard curve. The MC-TK-OFL standard curves at 300 nm were predetermined according to different MC-TK-OFL concentrations (R^2=0.9992). The drug loading content of MC-TK-OFL was calculated by the following formula: Loading content (%) = $(M_t - M_f) / M_n \times 100\%$, where M_t, M_f and M_n, represent the total mass of added MC-TK-OFL, the mass of MC-TK-OFL retrieved from the supernatant and the mass of NP-OFL, respectively.

Cytotoxicity of NP and NP-OFL

The cytotoxicity of NP and NP-OFL against human umbilical vein endothelial cells (HUVECs) was evaluated by MTT assay. Cells at a density of 5,000 per well were seeded in a 96-well plate and incubated for 24 h. After that, the culture medium was replaced with fresh medium containing different concentrations of nanogels (0, 10, 25, 50, 100, and 200 μg/mL). The cells were then incubated for another 24 h to assess the effects of the nanogels on cell viability.

***In vitro* drug release of NP-OFL**

The release behavior of ofloxacin from NP-OFL was investigated according to the standard curve of ofloxacin (R^2=0.9995). Initially, 2 mg of NP-OFL was dissolved in 2 mL of PBS. The resulting nanogel solution was then transferred into a dialysis bag with a molecular weight cut-off (MWCO) of 3500 Da. The dialysis bags were subsequently immersed in 20 mL of PBS containing different concentrations of H_2O_2 (0 mM, 0.25 mM, or 1 mM), and dialyzed under continuous shaking at 37 °C. At predetermined time intervals, 2 mL of the external solution was collected and 2 mL of fresh solution at the corresponding H_2O_2 concentration was added. The absorbance of the solution collected at the selected time points was measured by a UV spectrophotometer. Then, the accumulative release of ofloxacin was calculated at every time point according to the ofloxacin standard curve.

Characterization of BP samples

Glut, Glut-NP, and Glut-NP-OFL were cut into round patches of different sizes and randomly selected to study their properties. After lyophilization, the surface chemical components of BP samples (diameter of 8 mm) were characterized by an attenuated total reflection Fourier transform infrared spectrometer (ATR-FTIR, Thermo Fisher Scientific Nicolet iS50) and X-ray photoelectron spectroscopy (XPS, Thermo Fisher

Scientific K-Alpha). After lyophilization and subsequent gold coating, the morphology of BP samples (diameter of 8 mm) was observed by scanning electron microscopy (SEM, Thermo Fisher Scientific Apreo 2C) at an accelerating voltage of 10 kV. The distribution of the S element on BP samples was measured by an energy dispersive spectrometer (EDS).

Flow resistance test

To evaluate the mechanical stability and durability of the Glut-NP and Glut-NP-OFL coatings under conditions simulating physiological blood flow, a flow resistance test was conducted. Glut-NP and Glut-NP-OFL (diameter of 6 mm, n = 3) were mounted in a custom-made flow chamber connected to a peristaltic pump. The chamber was filled with PBS to simulate cardiac blood flow conditions, with the pump set to maintain a constant flow velocity of 40 cm/s, corresponding to physiological aortic flow rates. The samples were dynamically perfused at 37 °C for 72 h under continuous flow, then carefully retrieved, rinsed with PBS to remove debris, freeze-dried, and analyzed by SEM to assess coating stability.

***In vitro* cytotoxicity evaluation**

The cytotoxicity of BP samples was first evaluated via an extracting method. Glut, Glut-NP, and Glut-NP-OFL sterilized by ultraviolet irradiation (diameter of 10 mm) were incubated with 1 mL of DMEM (containing 5% fetal bovine serum) at 37 °C for 72 h, and the supernatant was collected for the cytotoxicity test. HUVECs were seeded in 96-well plates at a density of 5,000 cells per well and incubated for 24 h. Then, the old medium was replaced with 100 μL of supernatant extract, and the cells were cultured for another 24 h or 48 h, respectively. Finally, the relative cell viability was measured by CCK-8 (Cat No. 40203ES76, Yeasen, Shanghai, China) according to the kit instructions.

***In vitro* evaluation of ROS scavenging and macrophage polarization**

Raw 264.7 macrophages were seeded on sterilized BP samples at a density of 30,000 cells per well and cultured for 24 h. To induce inflammatory activation, LPS (100 ng/mL) was added for another 48 h. Subsequently, intracellular ROS levels were evaluated using DCFH-DA (10 μM) staining for 30 min at 37 °C, followed by observation via CLSM (λ_{ex} = 485 nm, λ_{em} = 500-550 nm). To further quantify inflammatory responses, culture supernatants were collected after LPS stimulation, and TNF-α secretion was measured using an enzyme-linked immunosorbent assay (ELISA) according to the manufacturer's protocol. For macrophage phenotype assessment, cells were fixed with 4% paraformaldehyde and immunofluorescently stained with anti-CD86 (M1 marker, red) and anti-CD206 (M2 marker, green) antibodies, with DAPI counterstaining for nuclei.

Determination of the hemolysis ratio

Glut, Glut-NP, and Glut-NP-OFL (diameter of 10 mm, n = 4) were placed in a 24-well plate and washed with PBS three times. Fresh rabbit blood (2 mL) was centrifuged at 1,500 rpm for 15 min, and the red blood cell (RBC) layer was collected and diluted with 40 mL 0.9% NaCl solution to obtain the RBC mixture. Then, 2 mL of RBC mixture was added to each sample and incubated at 37 °C for 1 h. After incubation, the RBC mixture was centrifuged at 3,000 rpm for 15 min, and the absorbance of the supernatant was measured at 540 nm. RBC mixture without incubation with the samples was used as the negative control, and RBC mixture containing 0.2% Triton X-100 was used as the positive control.

Platelet adhesion

Fresh rabbit blood was centrifuged at 1,500 rpm for 15 min to obtain the supernatant, platelet-rich plasma (PRP). Glut, Glut-NP, and Glut-NP-OFL (diameter of 6 mm) were placed on a 96-well plate and washed with PBS three times. Then, PRP (100 μL) was added to the samples and incubated at 37 °C for 2 h. Afterwards, the samples were washed with PBS three times and fixed with 2.5% (w/v) glutaraldehyde solution overnight, followed by washing with PBS thoroughly. After gradient dehydration and freeze drying, the number and shape of the platelets adhering to the surfaces of the samples were observed via SEM.

Whole blood adhesion assay

Glut, Glut-NP, and Glut-NP-OFL (diameter of 6 mm) were immersed in sterile PBS for 2 h and placed in a 96-well plate. Fresh rabbit blood (100 μL) was added to each sample and incubated at 37 °C for 1 h. The samples were then gently washed three times with PBS and fixed with 2.5% (w/v) glutaraldehyde solution overnight. After thorough washing to remove glutaraldehyde, the samples were dehydrated through gradient ethanol and freeze-dried for SEM observation.

Coagulation time

Glut and Glut-NP-OFL (diameter of 10 mm, n = 4) were incubated with 500 μL of porcine platelet-poor plasma (PPP) at 37 °C for 1 h. Following incubation, the plasma was collected, and the activated partial thromboplastin time (APTT), prothrombin time (PT), and thrombin time (TT) were measured using an automatic coagulation analyzer.

***Ex vivo* whole-blood circulation experiment**

After sterilization, Glut, Glut-NP, and Glut-NP-OFL samples (diameter of 6 mm, n = 3) were washed three times with PBS. The inner wall of the polyvinyl chloride (PVC) tubes was pre-treated with a heparin solution. Anticoagulated whole porcine blood was pumped into the PVC tubes using a peristaltic pump to establish a blood circulation

system, which was maintained for 1 h. Subsequently, the samples were removed, rinsed, fixed with glutaraldehyde solution, and dehydrated. The micromorphology of the samples was then observed via SEM.

Bacterial anti-adhesion test

First, Glut and Glut-NP-OFL (diameter of 10 mm, n = 3) were sterilized and placed in a 24-well plate. *E. coli* and *S. aureus* strains were incubated in LB media at 37 °C with shaking for 12 h to obtain a bacterial suspension of 10^7 CFU/mL. Subsequently, 1 mL of this bacterial suspension was added to each sample and incubated at 37 °C for 2 h. After incubation, the samples were rinsed three times with sterile normal saline to remove non-adherent bacteria, immersed in 5 mL of sterile normal saline, and subjected to ultrasonication for 5 min. Next, 20 μL of the resulting suspension was evenly spread onto nutrient agar plates and incubated at 37 °C overnight to acquire images and count the CFUs. For SEM observation, samples with adhered bacteria were fixed in 2.5% (w/v) glutaraldehyde solution at 4 °C overnight, dehydrated through a graded ethanol series and freeze-dried. In the SEM images, *E. coli* and *S. aureus* were highlighted using pseudo-coloring for clarity.

***In vivo* inflammation analysis**

To further investigate the anti-inflammatory potential of Glut-NP-OFL, both Glut and Glut-NP-OFL (diameter of 10 mm, n = 4) were sterilized and immersed in sterile PBS. Two male Sprague-Dawley rats (6–8 weeks of age, 200 ± 10 g) were anesthetized for subcutaneous implantation to assess the inflammatory response. After 7 days or 14 days post-implantation, the samples were retrieved and fixed in 4% paraformaldehyde solution overnight. Following fixation, the samples were dehydrated, embedded in paraffin, and sectioned. The expression of IL-1β and TNF-α was detected using the corresponding antibodies, and the ratio of IL-1β and TNF-α positive cells surrounding the samples was quantified using Image J software.

***In vivo* endothelialization analysis**

New Zealand white adult rabbits (2.5–3.0 kg) were anesthetized, and the femoral artery was surgically exposed. Glut and Glut-NP-OFL patches (2 mm × 10 mm) were sutured onto the vascular stent. Under guide-wire guidance, the stent-patch construct was introduced into the infrarenal abdominal aorta. After 21 days, the patches were harvested for CD31 immunofluorescence analysis to assess endothelialization.

***In vitro* calcification analysis**

Glut and Glut-NP-OFL (diameter of 10 mm, n = 6) were sterilized and mounted in a custom-built flow chamber connected to a peristaltic pump. An artificial calcium phosphate solution containing 1.5× the ion concentration of human plasma was circulated through the system to simulate pathological calcification conditions. The

flow rate was maintained at 40 cm/s to mimic cardiac blood flow velocity. The samples were dynamically perfused at 37 °C for 7 days, with daily cycling of 6 h flow-on and 18 h static incubation. After the assay, the samples were carefully rinsed with deionized water, freeze-dried, and analyzed by SEM coupled with energy-dispersive X-ray spectroscopy (EDS) to assess potential calcium phosphate deposition. In addition, selected samples were subjected to inductively coupled plasma optical emission spectrometry (ICP–OES) for quantitative analysis of calcium content.

***In vivo* calcification analysis**

Glut and Glut-NP-OFL (diameter of 10 mm, n = 6) were sterilized and immersed in sterile PBS. Three male Sprague–Dawley rats (3 weeks of age, 50 ± 5 g) were anesthetized by intraperitoneal injection of pentobarbital solution. Longitudinal surgical incisions were made along the midline of the rats' backs, and the samples were implanted into subcutaneous pockets on both sides of the incision. After 60 days, the implanted samples were retrieved and fixed in 4% (w/v) paraformaldehyde solution overnight. For histopathological examination, the fixed samples were stained with Alizarin Red to observe calcium deposition. For quantitative evaluation of the calcium content, the fibrous capsule surrounding the fixed samples was carefully removed. The samples were then freeze-dried, weighed, and dissolved in 5 mL of 6 M HCl. The calcium concentration in the resulting solution was quantitatively determined via inductively coupled plasma optical emission spectroscopy (ICP–OES).

Synthesis of MC-TK-OFL

The synthetic route of MC-TK-OFL is shown in Fig. S1.

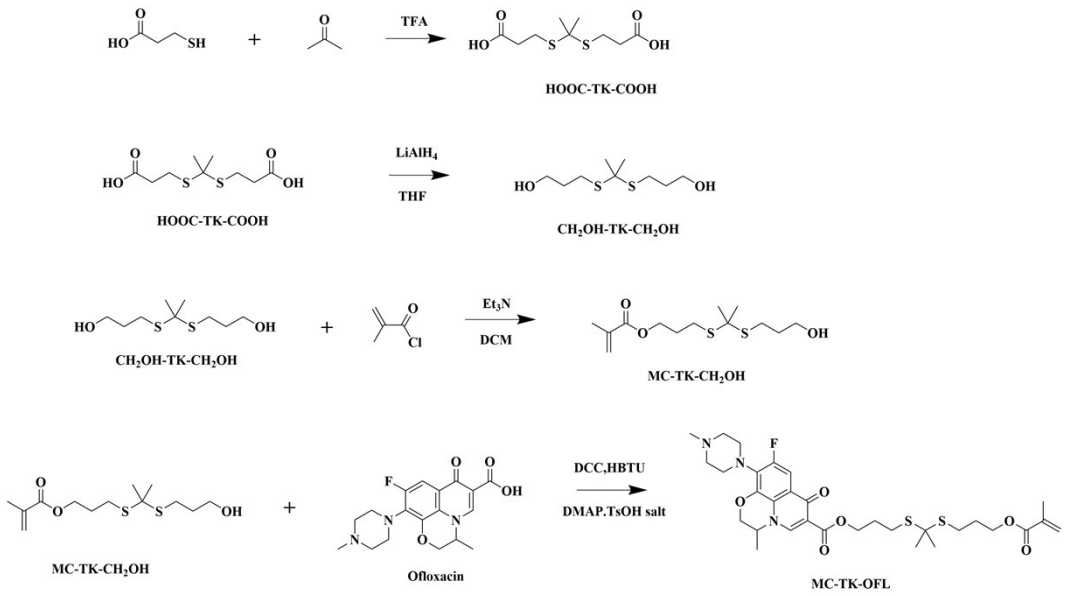

Fig. S1 Synthetic route of MC-TK-OFL.

Synthesis of 3,3'-(propane-2,2-diylbis(sulfanediyl))bis(propan-1-ol) (CH_2OH-TK-CH_2OH)

HOOC-TK-COOH was obtained according to a reported method [1–3]. CH_2OH-TK-CH_2OH was obtained according to a reported method [1].

Synthesis of 3-((2-((3-hydroxypropyl)thio)propan-2-yl)thio)propyl methacrylate (MC-TK-CH_2OH)

CH_2OH-TK-CH_2OH (5.00 g, 22.28 mmol) and TEA (3.38 g, 33.42 mmol) were placed in a round-bottom flask, and then 100 mL tetrahydrofuran was added. Subsequently, methacryloyl chloride (2.56 g, 24.51 mmol) in 20 mL tetrahydrofuran was added dropwise to the reaction mixture with an ice bath. After removing the ice bath, stirring was carried out for another 24 h at room temperature. The precipitate was removed by filtration and the solvent was removed under reduced pressure. The crude product was redissolved in DCM and extracted with NaCl solution three times. Afterward, the organic layer was collected, and the solvent was removed by rotary evaporation. Finally, column chromatography was used to purify the sample to obtain a viscous liquid MC-TK-CH_2OH. The ^{1}H NMR spectra of MC-TK-CH_2OH were gained on an NMR spectrometer (Advance Neo 400 MHz, Bruker, Germany) using DMSO-d_6 as solvent. ^{1}H NMR (400 MHz, DMSO-d_6) δ: 6.04-6.05 (m, 1H), 5.68-5.70 (m, 1H), 4.49-4.51 (m, 1H), 4.14-4.17 (t, 2H), 3.42-3.46(m, 2H), 2.64-2.68(t, 2H), 2.58-2.63(m, 2H), 1.84-1.92(m, 5H), 1.61-1.68(m, 2H), 1.54 (s, 6H) ppm.

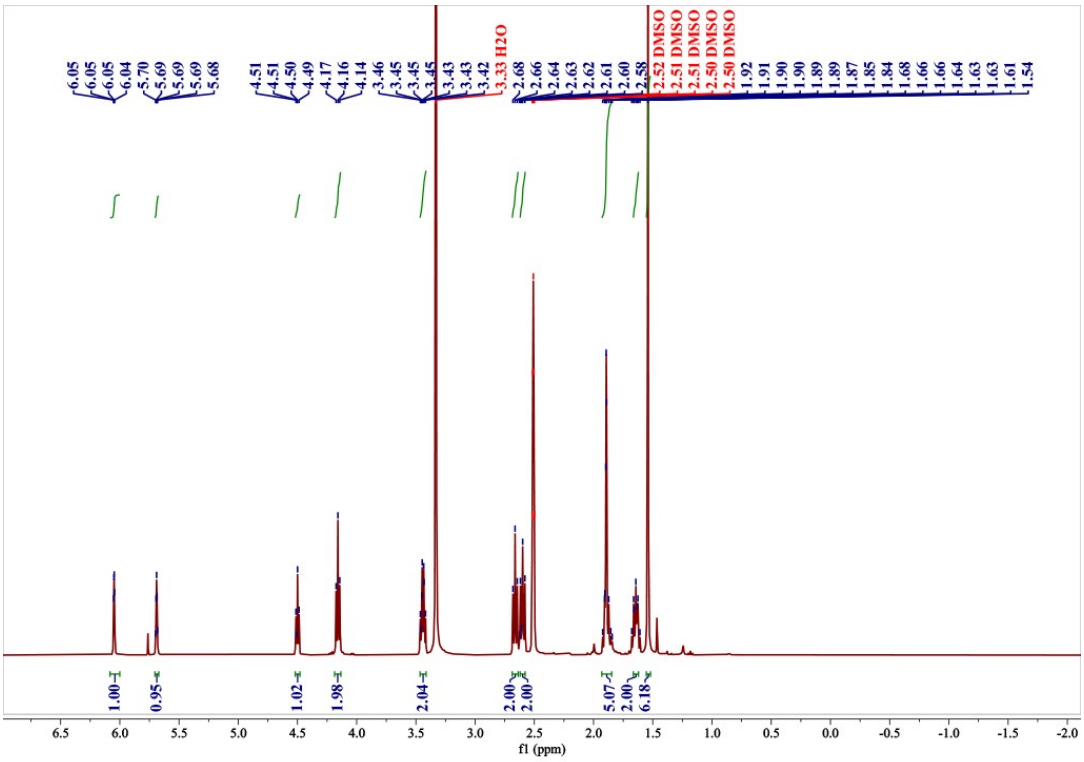

Fig. S2 ^{1}H NMR spectrum of MC-TK-CH_2OH in DMSO-d_6.

Synthesis of 3-((2-((3-(methacryloyloxy)propyl)thio)propan-2-yl)thio)propyl 9-fluoro-3-methyl-10-(4-methylpiperazin-1-yl)-7-oxo-2,3-dihydro-7H-[1,4]oxazino[2,3,4-ij]quinoline-6-carboxylate (MC-TK-OFL)

MC-TK-CH_2OH (0.50 g, 1.71 mmol), ofloxacin (0.62 g, 1.71 mmol), DMAP.TsOH salt (0.20 g, 0.68 mmol) and HBTU (0.84 g, 2.22 mmol) were dispersed in 20 mL DCM, and then DCC (0.46 g, 2.22 mmol) was added. Stirring was carried out for 48 h at room temperature. The resulting mixture was filtrated to remove the precipitate. Subsequently, the solvent was removed under reduced pressure, redissolved in DCM and washed with NaCl solution three times. The DCM phase was carefully collected, and the solvent was removed by rotary evaporation. Finally, the product was purified by column chromatography to obtain a pale yellow solid. The product was stored at -20 °C and labeled as MC-TK-OFL. The ^{1}H NMR and ^{13}C NMR spectra of MC-TK-OFL were gained on an NMR spectrometer (Advance Neo 400 MHz, Bruker, Germany) using DMSO-d_6 as solvent. ^{1}H NMR (400 MHz, DMSO-d_6) δ: 8.60 (s, 1H), 7.41-7.44 (d, 1H), 6.01-6.02 (t, 1H), 5.65-5.66 (m, 1H), 4.69-4.74(m, 1H), 4.49-4.53 (m, 1H), 4.30-4.34 (m, 1H), 4.21-4.25 (m, 2H), 4.12-4.15 (t, 2H), 3.23-3.27 (m, 4H), 2.73-2.76 (t, 2H), 2.65-2.69 (t, 2H), 2.44-2.47 (t, 4H), 2.25 (s, 3H), 1.84-1.96 (m, 7H), 1.57 (s, 6H), 1.40-1.42 (d, 3H) ppm. ^{13}C NMR (100 MHz, DMSO-d_6) δ: 166.24, 164.39, 146.01, 140.17, 135.62, 125.51, 123.67, 108.46, 103.65, 103.41, 67.86, 63.01, 62.47, 55.51, 55.07, 53.52, 49.83, 45.78, 30.46, 28.20, 27.93, 25.99, 25.85, 17.76, 17.52 ppm.

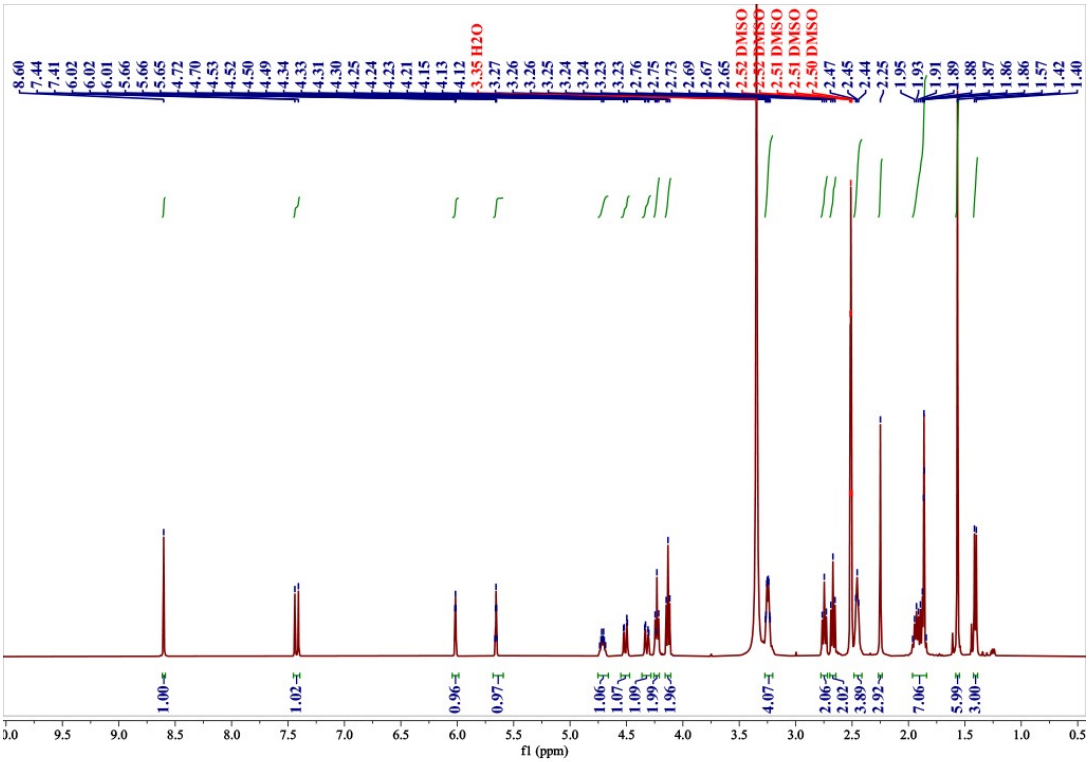

Fig. S3 ^{1}H NMR spectrum of MC-TK-OFL in DMSO-d_6.

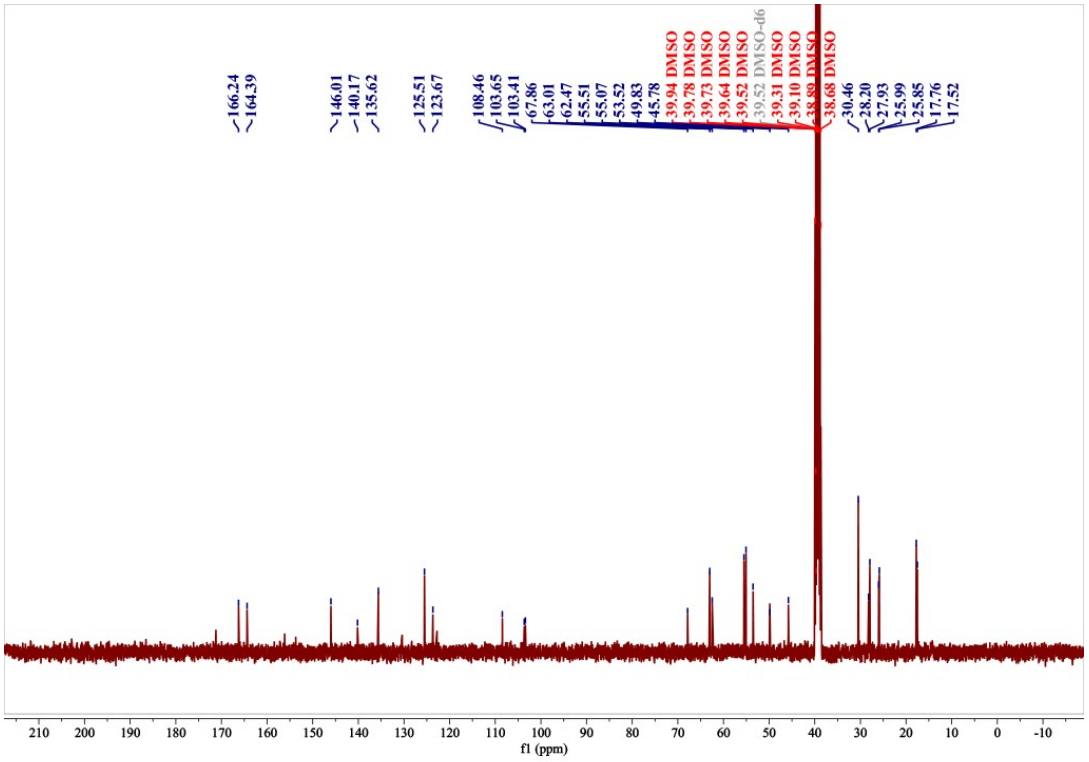

Fig. S4 ^{13}C NMR spectrum of MC-TK-OFL in DMSO-d_6.

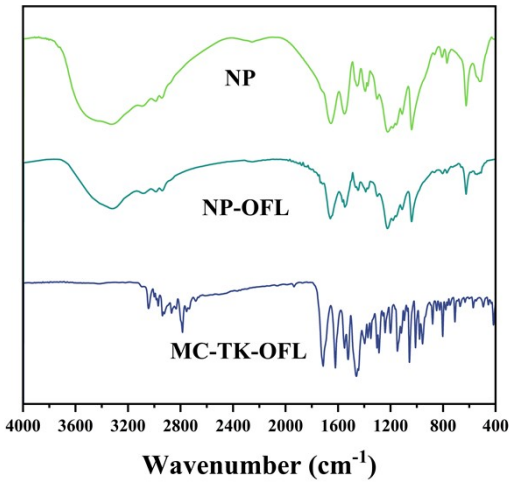

Fig. S5 FTIR spectra of NP, NP-OFL, and MC-TK-OFL.

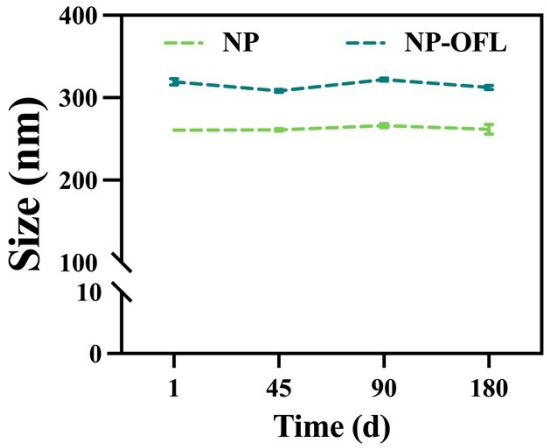

Fig. S6 Stability of NP and NP-OFL in PBS over time. n = 3.

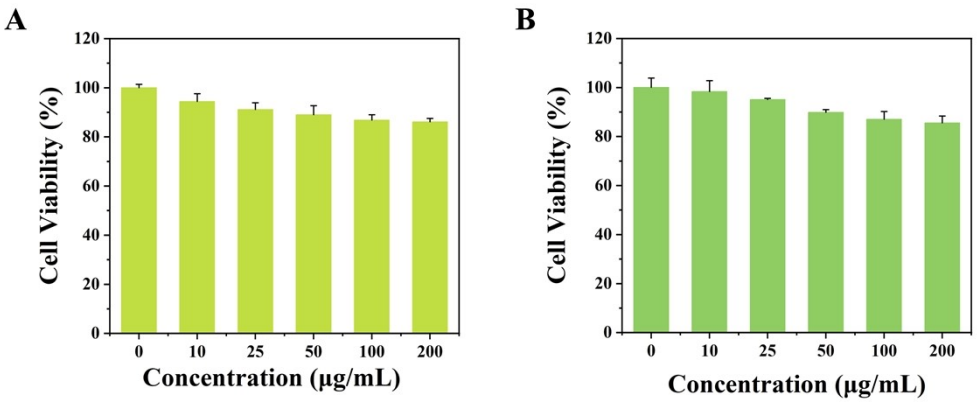

Fig. S7 Cytotoxicity of NP (A) and NP-OFL (B) against HUVECs. n = 3.

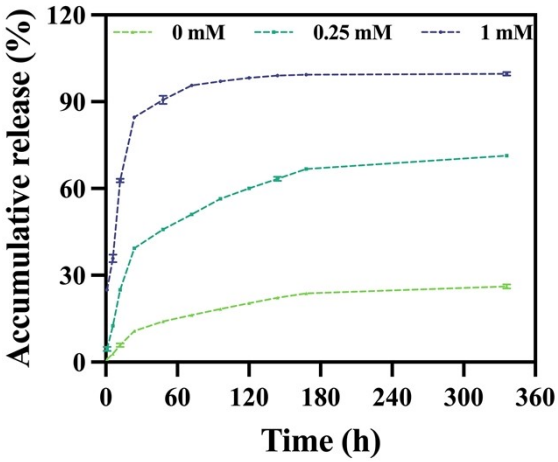

Fig. S8 Accumulative release curves of ofloxacin from nanogels under different H_2O_2 concentration. n = 3.

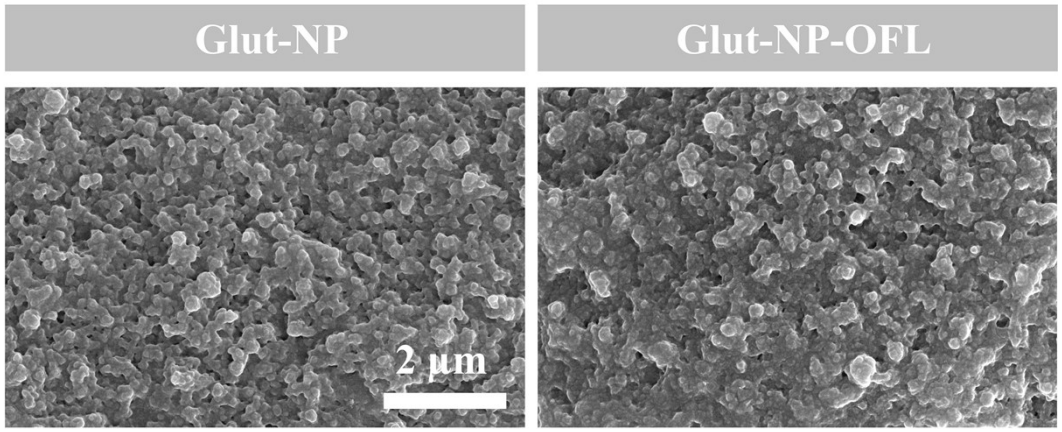

Fig. S9 SEM images after flow resistance test.

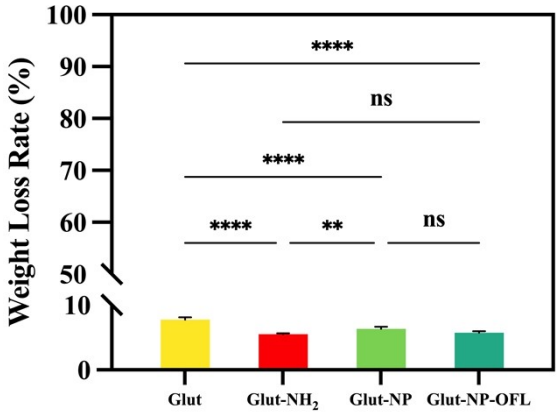

Fig. S10 Weight loss rate of BP samples after enzymatic degradation. n = 4.

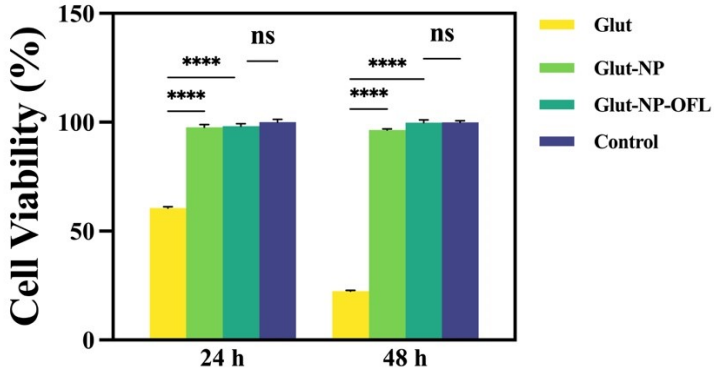

Fig. S11 Cell viability of HUVECs after incubation with the extracts of BP samples for 24 h and 48 h. n = 3.

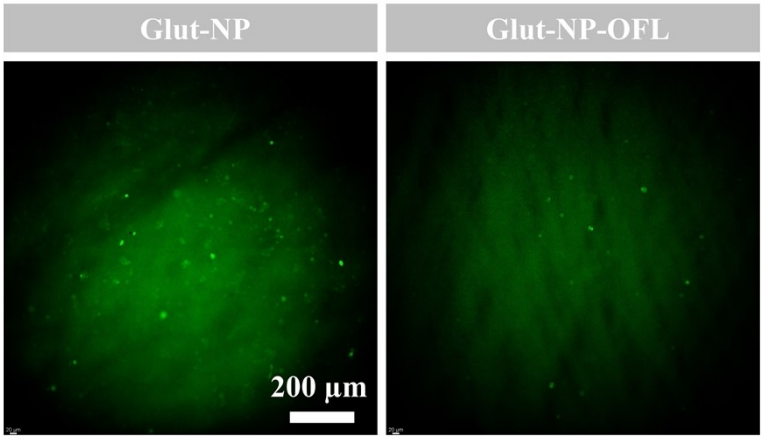

Fig. S12 Intracellular ROS in Raw 264.7 cells on Glut-NP and Glut-NP@OFL after LPS stimulation, visualized by DCFH-DA staining and CLSM.

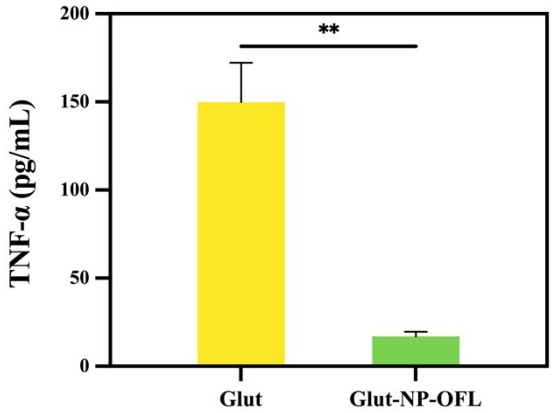

Fig. S13 TNF-α expression levels in Raw 264.7 cells cultured with Glut and Glut-NP@OFL measured via ELISA.

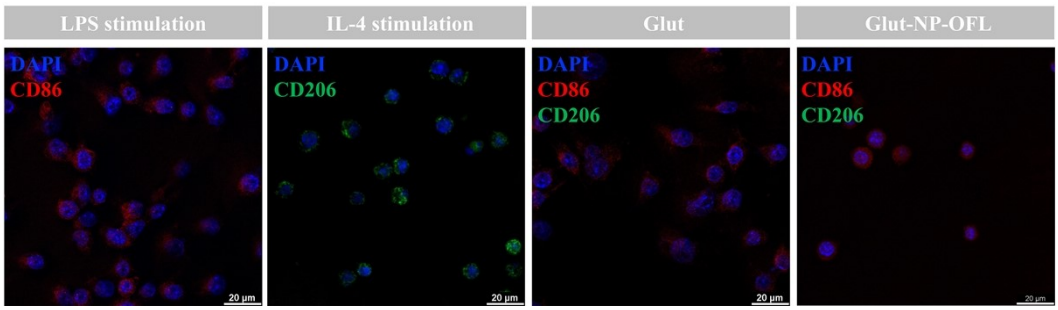

Fig. S14 Immunofluorescence staining of macrophage surface markers CD86 (M1, red) and CD206 (M2, green).

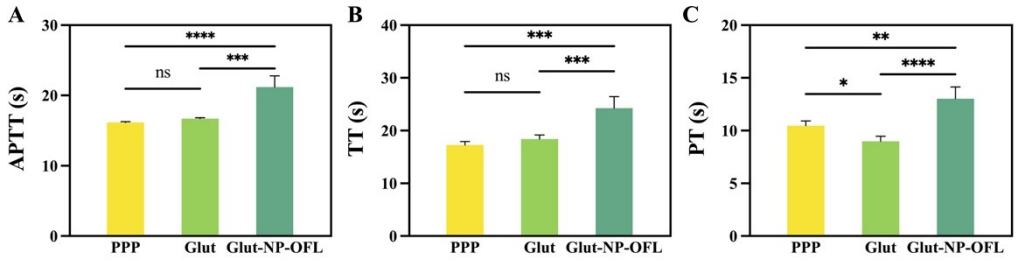

Fig. S15 Coagulation time of BP samples. n = 4.

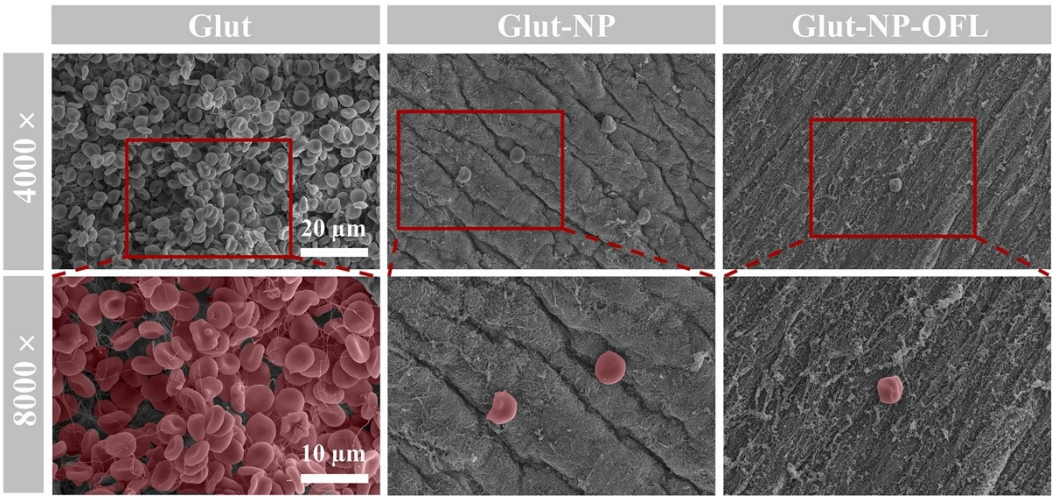

Fig. S16 SEM images of BP samples after *Ex vivo* whole-blood circulation experiment.

Fig. S17 Visual images of BP samples after AV-shunt experiment.

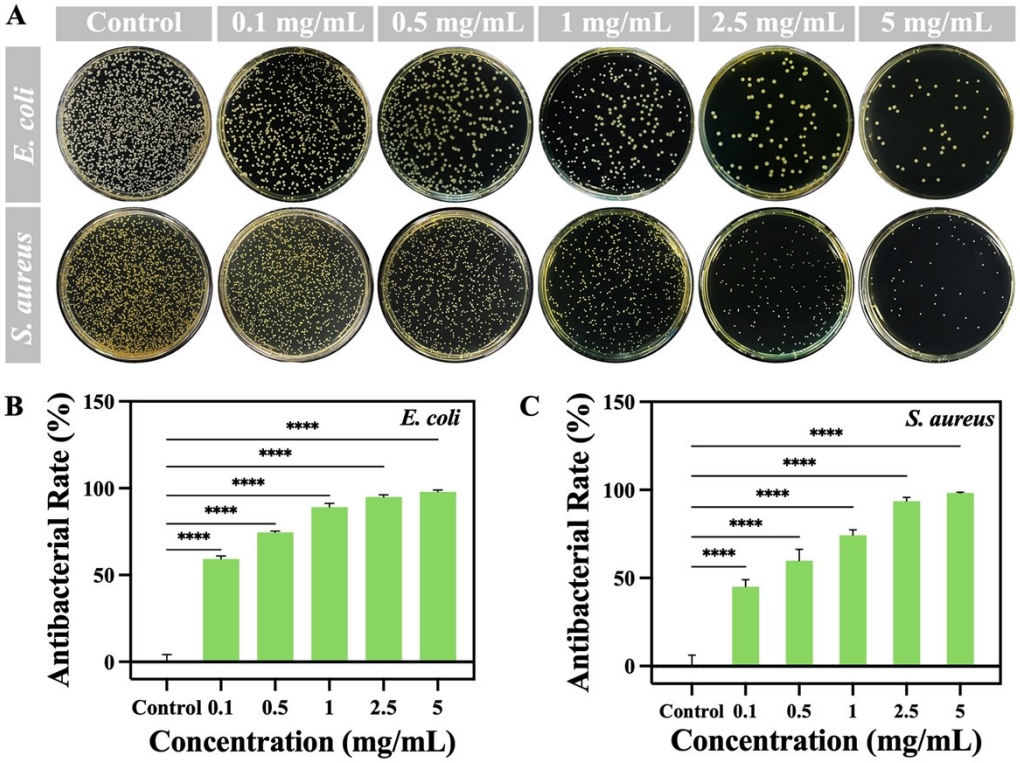

Fig. S18 (A) Visual images of colony-forming units after incubation with NP-OFL. (B) Antibacterial rate of different concentrations of NP-OFL against *E. coli*. n = 3. (C) Antibacterial rate of different concentrations of NP-OFL against *S. aureus.* n = 3.

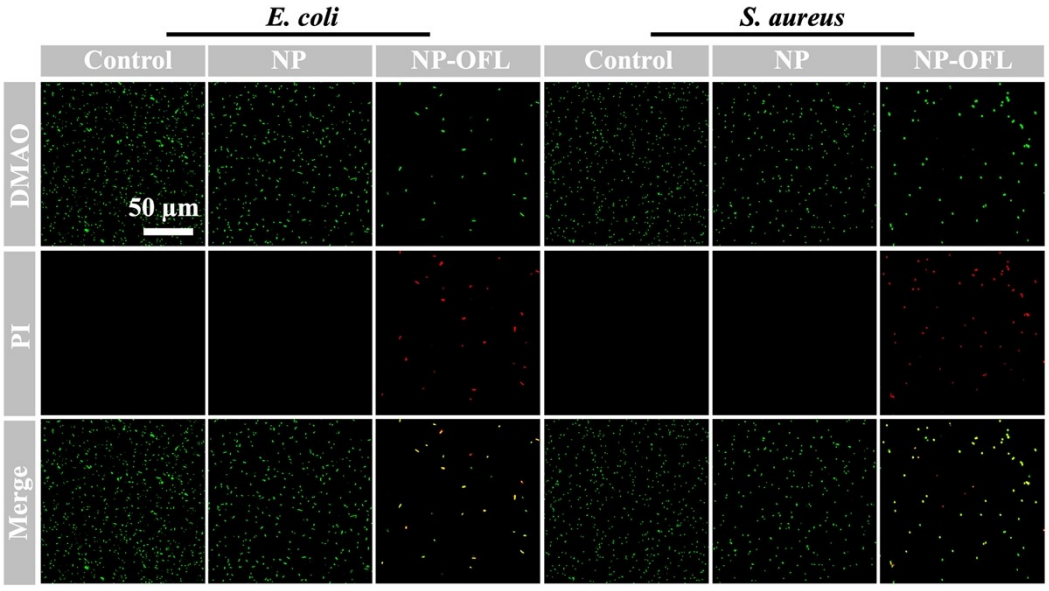

Fig. S19 LSCM images after incubation with NP and NP-OFL.

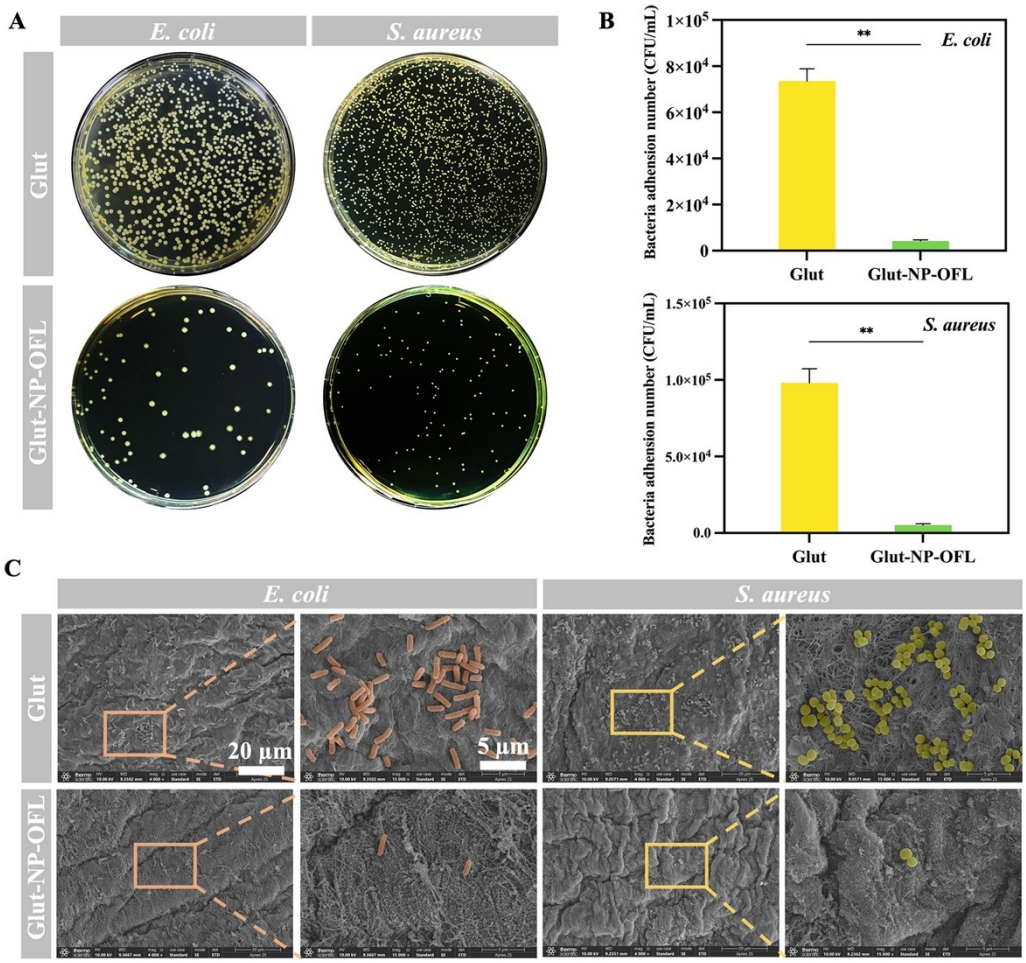

Fig. S20 (A) Visual images of colony-forming units. (B) The number of adhered bacteria on the surfaces of BP samples. n = 3. (C) SEM images of BP samples after bacterial adhesion experiment. Scale bars = 20 and 5 μm, respectively. (*E. coli* was marked in orange and *S. aureus* was marked in yellow).

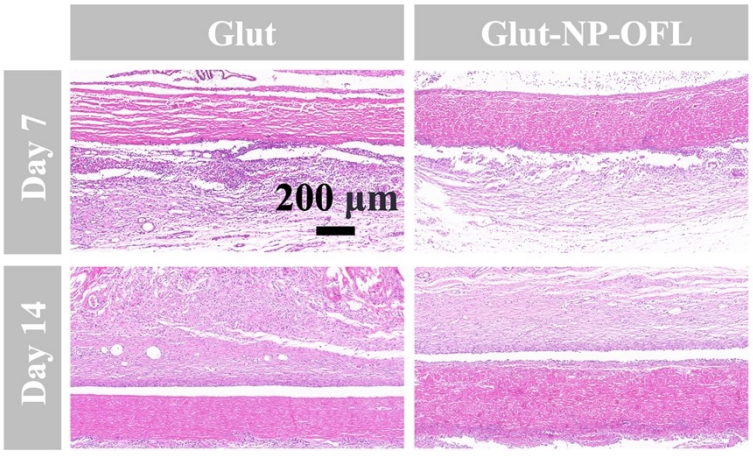

Fig. S21 H&E staining of BP samples after implantation for 7 or 14 days. Scale bar = 200 μm.

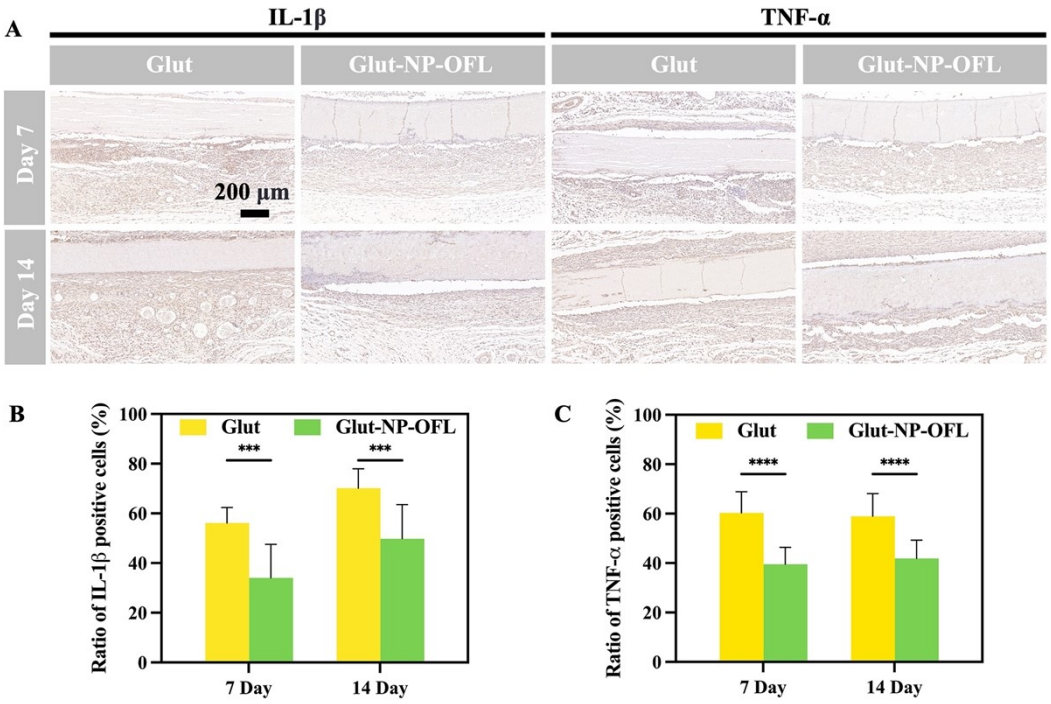

Fig. S22 (A) IHC staining of BP samples after implantation for 7 or 14 days. Scale bar = 200 μm. (B) Ratio of IL-1β positive cells of BP samples after implantation for 7 or 14 days. n = 10. (C) Ratio of TNF-α positive cells of BP samples after implantation for 7 or 14 days. n = 10.

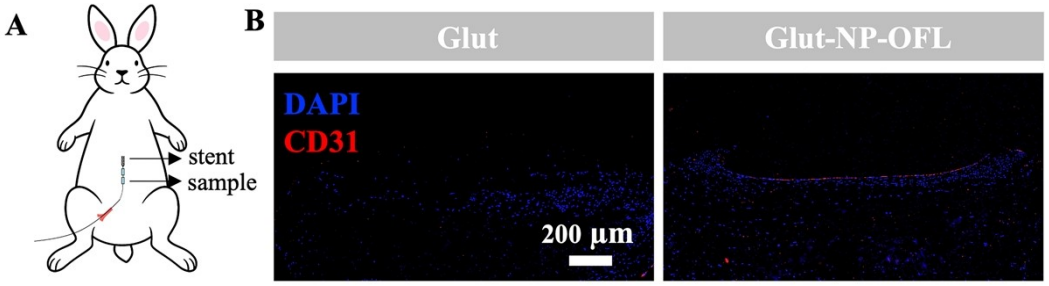

Fig. S23 (A) Schematic illustration of the surgical implantation procedure in the rabbit abdominal aorta model. (B) Representative fluorescence images of BP samples stained for nuclear marker DAPI (blue) and endothelial cell marker CD31 (red). Scale bar = 200 μm.

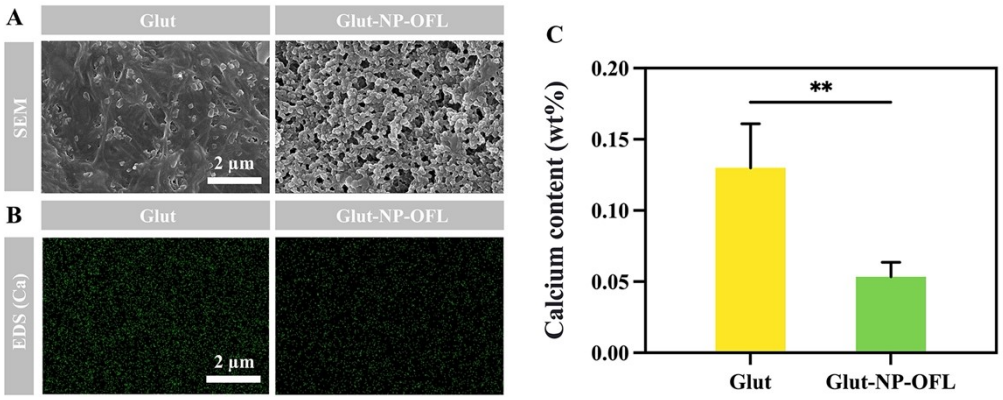

Fig. S24 (A) SEM images of BP samples after *in vitro* calcification assay. (B) Mapping diagram of Ca element on the surface of BP samples obtained by EDS. (C) Calcium content on the surface of BP samples obtained by EDS. n = 6. (D) Calcium content of BP samples obtained by ICP–OES. n = 3.

Reference

1 P. Li, Q. Liu, Z. Xiang, J. Wang, W.-X. Wu and W.-J. Yi, *Eur. Polym. J.*, 2023, **199**, 112473.

2 Q. Qiu, Y. Zhao, Y. Niu and H. Li, *Eur. Polym. J.*, 2024, **220**, 113470.

3 Yu. A. Davidovich and S. V. Kozlov, *Pharm. Chem. J.*, 2021, **55**, 506–509.